

Additive Manufacturing of Optical Waveguides

*Yushi Chu, Liling Dong, Yanhua Luo, Jianzhong Zhang
and Gang-Ding Peng*

Abstract

Optical waveguides play an important role in both scientific research and industrial applications. Additive manufacturing (AM) or three-dimensional (3D)-printing technology has great potential to revolutionize manufacturing of optical waveguides. AM offers a great opportunity in developing optical waveguides demanding new material compositions and structure designs for functionalities needed in fast-evolving modern applications such as Internet of things (IoT). These demands have become so diverse and sophisticated that the traditional waveguide manufacturing cannot meet. In this chapter, we briefly introduce optical fibers one of the most common typical optical waveguides and present the process and perspective of optical fiber fabrication by AM technology.

Keywords: waveguides, 3D printing, waveguides fabrication, 3D-printing silica optical fibers

1. Introduction

Optical waveguides have achieved great success in information transmission in the past decades, mainly due to the ultralow loss, large capacity, high power, and excellent mechanical robustness. Optical fiber as one of the most useful optical waveguides plays an essential role in telecommunications and forms today's Internet backbone. In this chapter, optical fiber is briefly presented in Introduction part, then some AM technologies are focused, and finally, the fabrications of optical fibers based on AM technology are introduced including the fabrication process and perspective.

Optical fiber is a flexible, transparent fiber made of glass or plastic that acts as a light-transmitting tool. Optical fiber usually consists of a core surrounded by a transparent cladding and a coating in order, shown in **Figure 1a**. The refractive index of the core is higher than cladding, creating the waveguide structure to transmit light by total internal reflection (TIR) as demonstrated in **Figure 1b**. Charles K. Kao firstly promoted that the loss of optical fiber could be reduced by removed impurities and applied as the communication medium when he worked at ITTT Standard Telephones and Cables in 1966. This pioneering work made him earn the Nobel Prize in Physics in 2009 [1–3]. However, it was impossible to fabricate ultrapure silica as Kao mentioned due to the technical limitation at that time. Fortunately, the first low-loss (20 dB/km

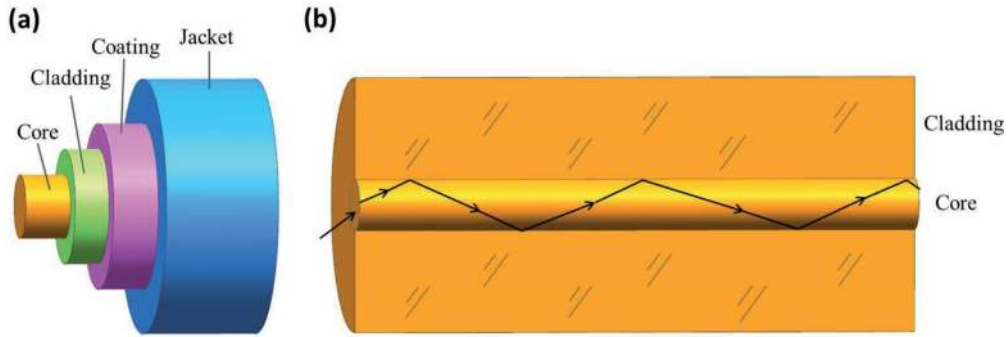


Figure 1.
(a) Diagram of typical optical fiber; (b) TIR in optical fiber.

at 632.8 nm) silica fiber was achieved by Robert D. Maurer from Corning in 1970 [4], and the modified chemical vapor deposition (MCVD) technology was invented by J. B. MacChesney from Bell Labs in 1974 [5]. Then, the optical fibers have developed rapidly and formed today's internet backbone. In 1999, Kao, Maurer, and MacChesney received the Charles Stark Draper Prize because of making the communication revolution possible [6].

Nowadays, there are some specialty optical fibers except the optical fiber for information transmission. The most representative ones are active fiber and microstructure optical fiber. For the active fiber, rare earth (RE) ions or metal ions are doped into optical fibers, generating luminescence under excitation, such as ytterbium (Yb) [7], erbium (Er) [8], thulium (Tm) [9], holmium (Ho) [10], and bismuth (Bi) [11]. Specific functions can also be achieved by codoping of two or more ions, for example, an ultra-broadband emission covering O-L telecommunication band was obtained from Bi/Er codoped optical fiber under 830-nm pumping, shown in **Figure 2a** [12, 13]. For the microstructure optical fiber, it usually consisted of one or more materials arranged periodically along the fiber length, realizing the refractive index modulation. The principles of light transmission are photonic bandgap effect and anti-resonance effect besides the TIR mentioned above. Microstructure optical fiber has many unique and novel physical properties, such as controllable nonlinearity, endless single-mode behavior, adjustable singular dispersion, low bending loss, and large mode field. **Figure 2b–e** shows the structures of typical PCFs [14–16].

The fabrication of optical fiber usually consists of two steps of preform manufacturing and fiber drawing, shown in **Figure 3**. The fiber drawing process is usually operated on a fiber drawing tower. The silica preform is heated to around 2000°C and becomes soft, then a thin bare fiber can be pulled out and cooled to solid, and finally, the bare fiber is coated and rolled into a coil, demonstrated in **Figure 3c**. For preform fabrication, chemical vapor deposition (CVD) is usually used for regular optical fiber, and microstructure optical fiber preform is manufactured by the stacking method. CVD utilizes SiCl_4 and GeCl_4 to oxidize into SiO_2 and GeO_2 at high temperature, which are deposited layer by layer onto the inner side of the quartz tube and sintered to form an optical fiber preform. According to the different deposition ways and heating source, CVD technologies can be divided into plasma chemical vapor deposition (PCVD) [17], outside vapor deposition (OVD) [18], vapor axial deposition (VAD) [19], and also MCVD [5] mentioned above. **Figure 3a** shows the schematic view of the four preform fabrication processes. Stack-and-draw method is usually used for PCF fabrication; glass capillaries

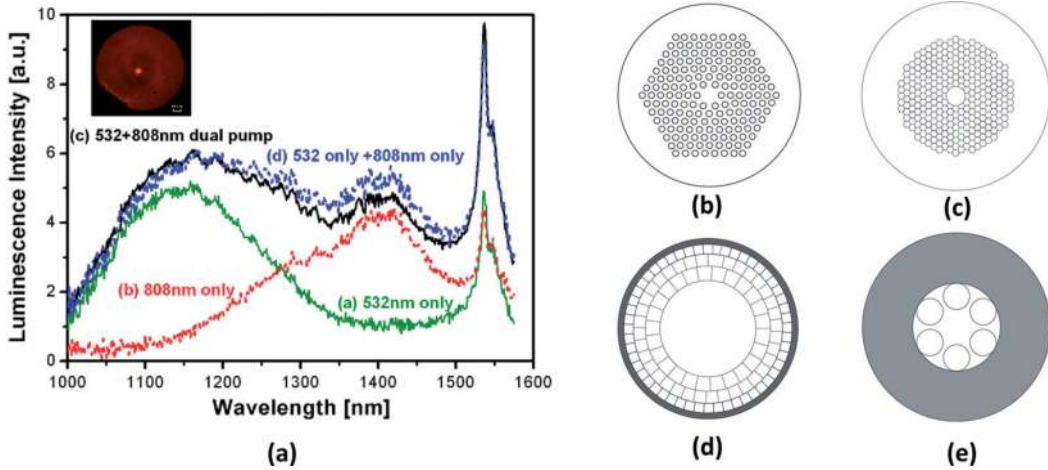


Figure 2. (a) Emission spectra of Bi/Er codoped optical fibers [12]; (b)-(e) structures of large mode area fibers, hollow core fiber, Bragg fiber, and anti-resonance fiber.

and rods of a specific size are stacked according to the designed structure as shown in **Figure 3b** and then drawn into PCF [20].

However, as the Internet has evolved into the ubiquitous Internet of things (IoT), the role of optical fibers is expanding from passive telecommunications transmission medium to lasers, sensors, devices, and beyond. This is creating the demand for

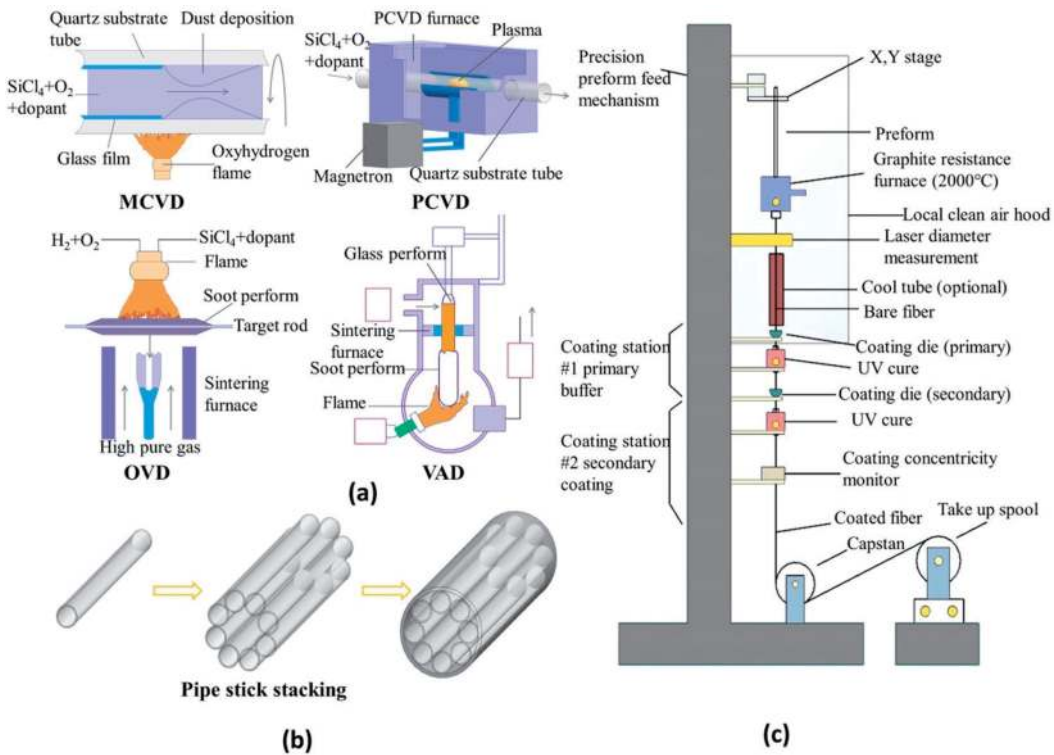


Figure 3. Optical fiber fabrication process, (a) preform fabrication-based CVD technology, (b) preform fabrication-based stack technology, (c) fiber drawing process.

increasingly sophisticated optical fibers. Unfortunately, the traditional fabrication technologies, for example, the CVD mentioned above, have limited capability in both material and structure flexibility for diverse and custom-designed functionalities. AM technology provides a solution to this problem.

2. Additive manufacturing technology

AM technology is a kind of rapid prototyping technology, also known as 3D-printing technology. It is a technique of constructing objects by layer-by-layer printing using bondable materials such as metal powder or plastic, based on a 3D digital model. Compared with traditional manufacturing methods, AM technology has outstanding performance in terms of economic cost, time efficiency, and customized design and has been successfully applied to various materials such as metals, polymers, metamaterials, and composite materials. These materials are shaped using different principles such as sintering, melting, extrusion, and laser/ultraviolet light curing, exhibiting different manufacturing accuracies, printing speeds, and resolutions. According to different materials, AM technology can be divided into solid-based AM technology and liquid-based AM technology, shown in **Figure 4**. For the solid-based AM technology, powder and filament are manufactured to objects by laser sintering/melting (selective laser sintering, SLS; selective laser melting, SLM) and nozzle extrusion (fused deposition modeling, FDM). For liquid-based AM technology, ink or photosensitive resin is shaped by gelation (direct ink writing, DIW) and light polymerization (stereolithography, SLA; digital light processing, DLP; and polymer jet, Polyjet). The above technologies have made great contributions to AM technology waveguides, providing new possibilities for the diversity of waveguide structures and functions.

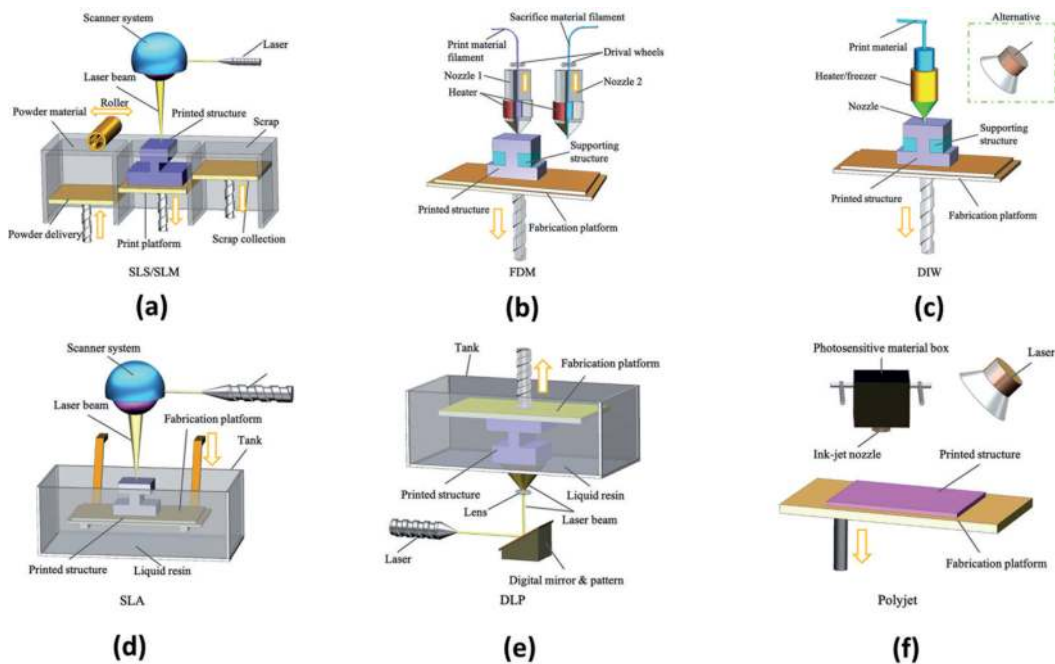


Figure 4. Classification and schematic diagram of AM technology, (a) SLS/SLM, (b) FDM, (c) DIW, (d) SLA, (e) DLP, and (f) Polyjet.

2.1 Powder-based additive manufacturing technology

SLS/SLM technology is a solid powder-based AM technology that uses a laser to selectively scan the powder bed and utilizes the interaction of the laser with the solid powder to sinter/melt loose powders together as shown in **Figure 4a** [21]. The basic bonding mechanisms of SLS/SLM include solid-state sintering, chemically induced bonding, liquid-phase sintering-partial melting, and full melting [22]. The essence of solid-state sintering is the thermal diffusion of the melting temperature of the material between the particles through heat transfer, which can realize the processing and combination of a variety of materials. When the laser-powder interaction time is short and no binder is present, a chemically induced bonding mechanism occurs, forming a new binder phase that helps facilitate the post-curing process. Liquid-phase sintering-partial melting occurs when insufficient laser heat is provided and only partial melting is achieved to obtain the bonding of structural particles. Full melting is mainly used in metal materials, which can directly produce nearly full dense materials without post-processing.

Compared with other AM technologies, the main advantage of SLS/SLM is the flexibility of material selection. Single-component powder particles, composite powder particles, mixtures of different powder particles, and different binder materials are all suitable for SLS/SLM. The size and shape of the particles directly determine the shrinkage, precision, and density of the constructed object [23, 24]. There are van der Waals forces between particles of smaller size, and it is easy to form agglomerates, which may directly lead to uneven dispersion of powder particles; while larger-sized particles directly affect the porosity, showing poor surface roughness, even significant cracking or delamination effects may form [25]. The quality of the constructed object is highly dependent on the correct choice of the processing parameter setting, such as laser power, layer thickness, scan speed, as well as hatch spacing [26]. Uniform particle size distribution and optimized processing parameters can effectively reduce the occurrence of “step effect” and shrinkage deformation and finally obtain a satisfactory SLS/SLM construction object [27].

2.2 Filament-based additive manufacturing technology

FDM—the most famous AM technology, belongs to filament-based technology, which is also one of the most widely used technologies in rapid prototyping technology. FDM uses a form similar to squeezing toothpaste to extrude material to build a layered structure. By heating the filamentous thermoplastic material, the nozzle extrudes the material along the printing path under computer control and deposits it on the hotbed. After one layer, the hotbed moves up the distance of one layer of material thickness and then prints the second layer; layer-by-layer deposition finally realizes the overall printing, shown in **Figure 4b** [21]. The key to FDM is the temperature at which the nozzle is heated. At higher temperatures, the viscosity of the filamentous material decreases, resulting in reduced accuracy and even collapse and deformation during the printing process; the filamentous material does not melt completely at lower temperatures, which is prone to delamination and even blocks the nozzle [28].

FDM has the characteristics of simple process flow, low cost, and low environmental requirements. It can also realize multi-material printing by switching nozzles. However, FDM also has disadvantages, such as low-printing accuracy, poor mechanical strength, and being prone to the “step effect” [28]. When using FDM to build an object with a certain degree of complexity, the support of supporting materials is

required to ensure the stability of the built part; otherwise, there may be collapse, which directly affects the manufacturing accuracy. In the actual construction process, the support structure can be printed with water-soluble filaments and then removed after post-processing, and the related problems caused by the support structure can be effectively reduced by optimizing the topology structure [29], optimizing the printing direction [30], and decomposing the printing structure to reduce the use of support materials [31].

2.3 Ink-based additive manufacturing technology

DIW technology is fabricated by layer-by-layer deposition, using an ink with shear-thinning properties that is extruded from a nozzle, shown in **Figure 4c**. The ink needs good viscoelasticity and fluidity to ensure smooth extrusion and maintain a good shape without clogging the nozzles. Because of the high accommodating capacity of ink materials, multi-component printing can be realized under the condition of meeting the basic requirements of ink, which can be widely used in many fields. Usually, the resolution of DIW technology is directly limited by the diameter and path of the nozzle. Latest studies have found that by adjusting the printing-related parameter set, it can successfully break through the constraints of line width and shape to achieve higher-resolution printing.

DIW technology has the advantages of simple process and multi-material printing, but there is also a disadvantage. Green bodies printed with DIW usually require long-term low-temperature drying to remove unnecessary solvents, so this step is critical to avoid cracks formed by drying.

2.4 Photosensitive resin-based additive manufacturing technology

SLA technology uses a laser with a specific wavelength to scan the photosensitive resin from point to line and to the surface according to the set path. After the layer is cured, move the worktable and apply a new layer of liquid resin on the surface of the original cured resin, so as to scan and cure the next layer, so that the newly cured layer can be firmly bonded to the previous layer. Repeating until the entire object has been fabricated, shown in **Figure 4d**. The key process parameters for SLA technology include initiator concentration, laser intensity, and scan rate. The initiator concentration and laser intensity directly determine the speed of the photopolymerization reaction, which in turn affects the processing efficiency. The spot size of the laser directly determines the resolution of the SLA [32]. Compared with FDM and SLS/SLM technologies, SLA shows better surface finish (nanoscale) and precision (micron scale), but the materials used are limited and it is difficult to achieve multi-material printing.

DLP technology is another AM technology that uses UV lamp curing. Its working principle is similar to SLA. The light source is changed from laser to UV lamp, and the introduction of digital micromirror devices (DMD) significantly shortens the construction time. The working principle of DLP technology is that the UV lamp is used as the light source, the three-dimensional CAD model is sliced through the software to form a two-dimensional dynamic mask pattern, and the sliced image is projected onto the surface of the photosensitive resin by DMD and cured, and the curing of one layer is completed, demonstrated in **Figure 4e**. The build plate is coated with a new layer of photosensitive resin, and the process is repeated layer by layer until the overall build is complete. DLP technology is one of the most widely

used rapid prototyping technologies [33]. Compared with SLA technology, DLP technology has the characteristics of fast printing speed, high printing accuracy, and uniform mechanical strength [34]. The curing depth is the key to the success of the layer connection. The setting of the layer thickness should be appropriately smaller than the curing depth to ensure the connection between each layer while avoiding the shrinkage and deformation problems caused by excessive curing and eliminating anisotropy [35].

Polyjet technology also uses UV lamp curing. Its working principle is that the nozzle controlled by the X-/Y-axis sprays photosensitive resin on the printing platform, and each layer of material is sprayed and irradiated with UV light for photocuring. After each layer is cured, the printing platform drops along the Z-axis direction, and the previous process is repeated until the printing is finished, exhibited in **Figure 4f**. Like the FDM technology, a support structure is usually required. The support material and the structural material are sprayed at the same time to achieve stable support for complex or overhanging structures. The support materials are generally water-soluble materials, which are easy to remove later [36]. Polyjet technology has many advantages of rapid prototyping manufacturing, providing good surface finish, high precision and layer resolution, high printing efficiency, and also enabling multi-material printing.

3. Optical fiber fabrication by additive manufacturing technology

With the rapid development of modern technology and application fields, the requirements for optical fibers in terms of structure and materials are more complex and diverse, striving to achieve the customized structural design and free and flexible material combinations. However, traditional optical fiber manufacturing methods such as CVD or stack-and-draw are difficult to meet this demand. Optical fiber manufacturing based on CVD processes is limited by the lathe itself, which has limited structural flexibility, and it is difficult to realize the manufacture of complex optical fiber structures, and it is necessary to maintain a highly uniform radially symmetrical temperature and pressure during the manufacturing process [37]. Although the stack-and-draw can achieve a certain degree of structural complexity, the flexibility of materials is limited, and it is very time-consuming and labor-intensive [38]. AM technology provides huge opportunities for the development of new cylindrical fibers such as new structural fibers.

3.1 Polymer optical fiber fabricated by additive manufacturing technology

Polymer optical fibers (POFs) are ideal materials for short-range communications and are increasingly used due to their low cost and high elastic strain limit. POF is usually fabricated by extrusion or drilling method, until Cook et al. reported that POFs were fabricated using FDM 3D-printing technology in 2015 [39]. The commercially available 3D-printing filament consisting of a propriety polystyrene mixture containing styrene-butadiene-copolymer and polystyrene was used as the raw materials. An optical fiber geometry consisting of a solid core surrounded by six air holes was chosen as an example and shaped to preform by FDM 3D printer, as shown in **Figure 5a**. The preform was then annealed and drawn to fibers. The light-guiding images of fiber end faces at 630 nm and 515 nm, white-light output projected onto a screen, and the relative schematic setup are demonstrated in **Figure 5b**. The

loss of the as-made POF was ~ 1.5 dB/cm, ~ 0.75 dB/cm, and ~ 1.51 dB/cm at 632 nm, 1064 nm, and 1550 nm, respectively.

Compared with the traditional POF manufacturing technology, the optical fiber preform manufactured by AM technology greatly simplifies the manufacturing process and saves a lot of time and labor costs. In addition, due to the integrated manufacturing, the waste of materials caused by drilling and other methods in the traditional manufacturing process is avoided. Despite the great advantages of using AM technology to manufacture preforms, the loss of manufacturing optical fibers is still high. These losses mainly come from the scattering caused by the gap between layers during the printing process, which can be reduced by an additional annealing process or optimized fiber drawing process [39].

After the first demonstration of POF by AM technology, various types of POFs fabricated by AM technology were reported, such as terahertz (THz) fiber, photonic bandgap fibers, anti-resonant fibers, Bragg fibers, step index fiber with two materials, and magnetically doped fiber with multi-materials by FMD, DLP, STL, and Polyjet methods [40–46].

3.2 Silica optical fiber fabricated by additive manufacturing technology

Although POFs realize low-cost AM technology and are widely used in short-distance communication, silica fiber plays an irreplaceable role in the long-distance transmission process. Besides, silica material has unparalleled optical transparency, excellent electrical insulation, chemical resistance, and thermal stability. How to break through the traditional silica fiber manufacturing method and realize the AM of silica fiber has become a problem worthy of further study. In 2016, F. Kotz et al. proposed a soft lithography method and successfully mixed silica nanoparticles with monomer solution, combined with light curing to prepare “liquid glass,” which provided a new way for silica glass fabricated by AM technology [47]. After that, the combination of organic matter and silica has been widely used in the AM of silica glass. For example, in order to bridge the gap between fused silica glass and polymer processing,

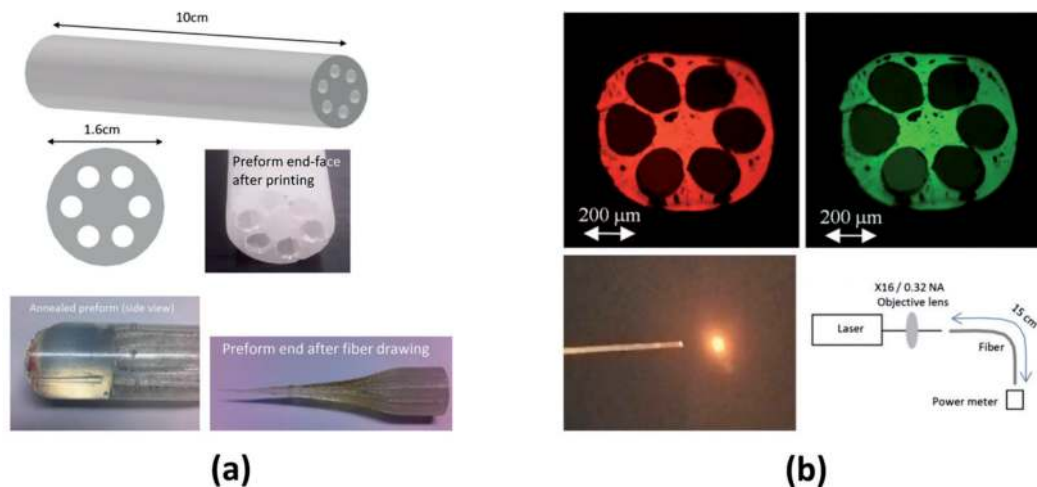


Figure 5. (a) Illustration of POF preform design, photos of annealed preform and preform after fiber draw. (b) The light-guiding images of fiber end faces at 630 nm and 515 nm, white-light output projected onto a screen, and relative schematic setup.

“Glassomer” was introduced, which successfully combined the advantages of polymer processing with the excellent material properties of fused silica glass, which was heat treated to form the same optical properties as commercial fused silica glass [48]. Based on the previous two methods, the organic-inorganic hybrid photosensitive resin was prepared, and optical glass was successfully printed by DLP technology [49]. In addition, the use of DLP technology to induce the phase separation of the photosensitive resin provides the possibility for the fabrication of complex structures, and multi-component glass [50]. Lawrence Livermore National Laboratory (LLNL) has also developed a similar organic-inorganic hybrid silica material with sol-gel ink, silica glass printed by DIW technology, and optical glass doped with Ti and Ge [51–53].

3.2.1 Silica fiber fabrication based on DLP technology

The above-mentioned technologies for AM of silica glass lay the foundation for the AM of silica optical fibers. However, the size of silica glasses produced by AM was small, usually only 10 millimeters, which was far from the size of the optical fiber preforms. The main reason may be that the size of the preform is large, impurities are likely to remain in the preform after debinding, and the cooling rate after sintering is too slow, resulting in crystallization or ceramicization, and the overall devitrification of the preform. In response to this problem, Chu. Y et al. optimized the method and successfully used DLP AM technology to manufacture traditional single-mode fiber and multimode fiber in 2019 [54]. Then, the research group continued their work and fabricated multi-component and multicore optical fibers using DLP 3D-printing technology [55]. The process of bismuth and erbium codoped optical fiber (BEDF) manufactured by AM technology is shown in **Figure 6**.

Firstly, silica nanoparticles were dispersed into a UV photosensitive monomer forming a stable photosensitive resin. Secondly, the pre-designed optical fiber preform was printed by DLP printer, and functional materials such as Ge^{4+} , Er^{3+} , and Bi^{3+} were doped into the core. Ge^{4+} was used to adjust the refractive index to realize the waveguide structure, but Er^{3+} and Bi^{3+} were utilized to achieve the broadband near-infrared luminescence, presented in **Figure 6a–c**. Thirdly, the printed preform was moved to a furnace to remove the organic components and achieves densification. The temperature setting is shown in **Figure 6d**, the mass and size change clearly pointed out that the organics were removed before 600°C and the preform started to densify after 600°C . Finally, the preform was drawn to the fiber at 1855°C . Before drawing, the preform was heated to 810°C and kept for 3 hrs for removing the moisture absorbed by the preform due to the porous structure during storage.

The drawn fiber was characterized by X-ray diffraction (XRD) using the powdered BEDF without coating, and the pattern pointed out that the fiber was amorphous, shown in **Figure 6e** inset. The cross-sectional microscopy images and electron probe micro-analysis (EPMA) of BEDF are shown in **Figure 6f** and **Figure 6g**, respectively. Although the crack and shrinkage were noticed, multicore structures were kept. Elements distribution of BEDFs was as expected, resulting in a refractive index difference between the core and cladding to form the waveguide structure, shown in **Figure 6g–i**. The loss and emission spectra of BEDF are demonstrated in **Figure 6j–k**. Typical characteristic peaks of bismuth and erbium were clearly identified.

DLP additive preform manufacturing has received attention from peers. In 2021, Zheng et al. have made progress in the AM of microstructured optical fibers; a ytterbium-doped microstructured optical fiber preform with a diameter of about 12 mm and a length of 20 mm was fabricated. The preform was then drawn to fibers,

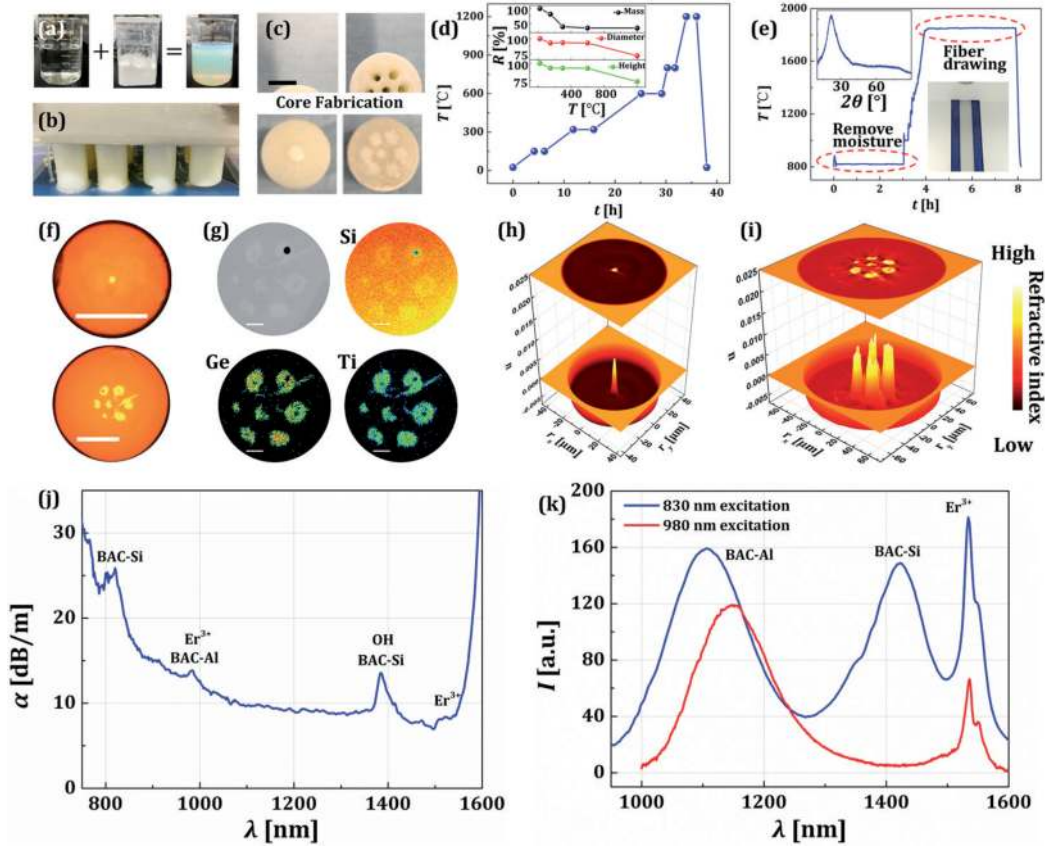


Figure 6.

(a) Dispersion of silica nanoparticle into ultraviolet curable resin, (b) preform cured by DLP 3D printing with UV light at 385 nm, (c) preforms before and after core filling, the scale bar is 10 mm, (d) temperature setting of the preform debinding process, inset is the remaining ratio of mass and size during the debinding process, (e) temperature change of the fiber drawing process. Inset is the XRD pattern of the drawn fiber and the photo of the drawing tower, (f) fiber cross-sectional images recorded by a microscope with a 50- μ m scale bar; (g) cross-sectional view of seven-core BEDF, and EPMA-WDS mappings of different elements from the cross section (scale bar: 10 μ m), (h)-(i) three-dimensional refractive index profiles of single- and seven-core BEDF, (j) loss spectrum of the single-core BEDF, (k) emission spectra of a single-core BEDF excited by the 830-nm and 980-nm lasers [54, 55].

the core was doped with 0.1 wt% ytterbium oxide, and six air holes were evenly distributed in the cladding [56]. The relevant information is shown in **Table 1**.

However, there are several difficulties in the process of printing silica fiber with DLP technology:

1. Due to the small particle size distribution of silica nanoparticles, clusters are prone to occur. It is necessary to ensure that the silica nanoparticles are evenly dispersed in the UV photosensitive resin to avoid scattering caused by particle accumulation; at the same time, it is necessary to ensure the stable suspension of silica nanoparticles for several weeks, to avoid the sedimentation of silica due to long-term placement under the influence of gravity, especially in the case of high solid content.
2. The correct selection of the printing parameter is the key to the AM process. The determination of layer thickness is closely related to the irradiation dose, $C_d = D_p \ln(E/E_c)$, where C_d is the depth of cure, E is the exposure energy, E_c is the critical exposure energy, and D_p is the depth of penetration [60]. A semi-

empirical formula suggests that the layer thickness should be slightly lower than the cure depth to ensure a close connection between the layers. In addition, attention should be paid to the balance between printing efficiency and layer thickness exposure time parameter selection while ensuring successful printing.

3. In the heat treatment process, the choice of heating rate and temperature is decisive. High transparency and compactness are guaranteed with all organics removed, and cracks during debinding and anisotropy due to non-uniform shrinkage are avoided as much as possible.
4. Controlling the fiber drawing parameters during the fiber drawing process can effectively avoid collapse and deformation, for example, the fiber drawing temperature directly determines the surface tension and viscosity of the fiber.

AM	Year	Preform		Fiber			References	
		Type	Size (mm)	Type	Size (μm)	Materials		Loss (dB/m)
DLP	2019	Solid	D: 25 L: 50–100	SM	d: 131 d_c : 4	M_{Clad} : SiO ₂ M_{Core} : SiO ₂ - GeO ₂ -TiO ₂	13.4@532 13.9@660 114@1550	[54]
			D: 25 L: 50–100	MM	d: 242 d_c : 14	M_{Clad} : SiO ₂ M_{Core} : SiO ₂ - GeO ₂ -TiO ₂	11@1300 5.8@1550	
	2021	Micro- Stru.	D: 12 L: 20	—	d: 110 d_c : -	M_{Clad} : SiO ₂ M_{Core} : SiO ₂ : Yb	11@800 14@1100	[56]
			D: 22 L: 40–100	SM	d: 80 d_c : 3.5	M_{Clad} : SiO ₂ M_{Core} : SiO ₂ - GeO ₂ -TiO ₂ : Al/Bi/Er	9.6@1300 6@1550	
	2022	Solid	D: 22 L: 40–100	7 cores	d: 150 d_c : 3–11	M_{Clad} : SiO ₂ M_{Core} : SiO ₂ - GeO ₂ -TiO ₂ : Al/Bi/Er	10.7@633	[55]
			D: 2 L: 7	MM	d: 100 d_c : 40	M_{Clad} : Fluoride M_{Core} : SiO ₂ : Er	63@980 152@1535	
SLS	2019	Solid	D: 12 L: -	MM	d: 200 d_c : -	M_{Clad} : SiO ₂ M_{Core} : SiO ₂	23@800 28@1100	[58]
		Micro- Stru.	D: 40 L: -	—	—	—	—	
	2020	Solid	D: 18 L: -	—	d: 150 d_c : 11	M_{Clad} : SiO ₂ M_{Core} : SiO ₂ -GeO ₂	8.32@800 24@1100	[59]
		Micro- Stru.	D: 38 L: -	—	—	—	—	

Table 1. Additive manufacturing on silica optical fibers (Micro-Stru.: micro-structure, D: outer diameter of preform, L: length of preform, SM: single mode, MM: multimode, d: diameter of optical fiber, d_c : diameter of fiber core, M_{Clad} : material of fiber cladding, M_{Core} : material of fiber core).

3.2.2 Silica fiber fabrication based on DIW technology

At present, silica fiber preforms can also be made by DIW AM technology using inks mixed with silica and organics besides the DLP method. Erbium-doped optical fiber (EDF) was reported by the University of Southampton using DIW method [57]. Hydrophobic fumed silica and erbium chloride were doped in organics, such as tetraethylene glycol dimethyl ether and polydimethylsiloxane, to form the ink. Then, the ink was printed layer by layer with a printing speed of 40 mm/s at room temperature, and each layer was fixed at 500 μm . The printed rod was debinded and consolidated to glass. Finally, the glass rod was inserted into a fluorinated tube and drawn to EDF, and the fluorinated tube was used to provide the refractive index contrast, resulting in the waveguide structure. The typical absorption peaks of erbium were clearly observed at 980 nm and 1535 nm with the absorption of 62.98 dB/m and 151.49 dB/m, respectively. In addition, the overall absorption was still notable mainly due to the residual OH, PDMS, and impurities from the starting materials.

3.2.3 Silica fiber fabrication based on SLS technology

The use of SLS technology to print silica optical fibers fully utilizes the advantages of SLS technology in producing complex geometric shapes and multi-component printing. Optical fiber preforms with various structures and multi-components are formed by selectively scanning powder layers layer by layer with a CO_2 laser beam [58]. Microstructured fibers and anti-resonant fibers were printed by SLS technology. In order to evaluate the performance of the printed silica, a solid preform with 12 mm diameter was printed and inserted into a glass tube and drawn to fiber. A refractive index difference of 4×10^{-4} was achieved between the printed preform and glass tube. The attenuation of the optical fiber was measured in the range of 600–1150 nm, and the lowest attenuation was 23 dB/m around 800 nm. The high attenuation was mainly induced by the purity of the starting silica powder and parameters setting during the 3D-printing process.

After a series of SLS manufacturing technology optimization, photonic crystal fiber, anti-resonance fiber, and multicore Ge-doped optical fiber preforms were successfully fabricated by the same research group. The multicore Ge-doped optical fiber realizes a waveguide structure with a step index of refraction, and the lowest loss after the drawing reduced to 8.32 dB/m around 800 nm. Experiments have proved that the transmission loss can be effectively reduced by optimizing the powder characteristics and printing parameters [59].

4. Conclusions

In this chapter, we mainly introduced the fabrication of optical fibers using additive manufacturing technology and briefly presented the basic concepts of optical fibers and typical additive manufacturing techniques. Compared with traditional waveguide manufacturing techniques, such as CVD, additive manufacturing technology has higher manufacturing precision and manufacturing efficiency and lower manufacturing costs. At the same time, additive manufacturing technology exhibits unparalleled flexibility in structural and material designs that is essential to the realization of new and multifunctional optical fibers and devices.

At present, the additive manufacturing of polymer optical fiber preform mainly includes melt extrusion and light curing. Although the melt extrusion method has relatively low cost, the resolution of the manufacturing preform is low. While the light-curing technology is just the opposite. The manufacturing cost is higher than that of melt extrusion, and the resolution is also high, which is suitable for manufacturing preform with complex structures, such as bandgap optical fiber preform.

For the silica optical fiber preform, there are two main additive manufacturing methods. The first method is to combine silica and organic matter to form the resin, then use additive manufacturing technologies, such as light or heat curing, to shape, and finally obtain the optical fiber through debinding, sintering, and fiber drawing. This manufacturing method has a very high fabricating resolution and becomes the main way of additive manufacturing of silica optical fiber preform. However, due to the introduction of organic matter, an additional debinding process is required in the later stage, even if a small amount of organic matter remains, it will cause high loss. The second method is to directly sinter or melt the silica powder by laser. This method can effectively avoid the organic matter, but its development is also restricted by the problems of manufacturing accuracy and ceramics caused by phase transformation. The technologies above make full use of the advantages of additive manufacturing technology in molding, such as short time, low labor cost, and low material cost, and fully reflect its potential in the manufacturing of complex geometry silica optical fiber.

Although optical fiber fabricated by additive manufacturing has so many advantages, loss, manufacturing size, and multi-materials are still the factors limiting its development, and it is also the research direction in future. For the loss of additive manufacturing optical fiber, especially for the silica optical fiber, the loss mainly comes from microbubbles, microcracks, stripes between layers during printing, organic matter not removed during debinding process, and the purity of raw materials. For the manufacturing size, the main problems rise from the loss caused by incomplete removal of internal organic matter during debinding due to the large size of preform, and the cracking caused by uneven stress distribution during debinding, sintering, or cooling process. For the additive manufacturing of multi-material optical fiber, the integration of glass, semiconductor, crystal, metal, or polymer into the so-called hybrid fiber is also another research focus of additive manufacturing of fibers, and the key point is how to balance the relationship between melting point and thermal expansion coefficient of each material. At present, a large number of researchers have carried out systematic research on the above problems. We have reason to believe that just like the development trend of traditional optical fiber, the optical fiber fabricated by additive manufacturing will also experience the development trend of reducing loss, multi-structure, and multi-material and bring revolutionary changes to the optical fiber manufacturing industry with its unparalleled advantages.

Author details

Yushi Chu^{1,2}, Liling Dong^{1,2}, Yanhua Luo³, Jianzhong Zhang^{1*} and Gang-Ding Peng³


1 Key Laboratory of In-fiber Integrated Optics of Ministry of Education, College of Physics and Optoelectronic Engineering, Harbin Engineering University, Harbin, China

2 Fiber Optical Sensing Center for Excellence, Yantai Research Institute, Harbin Engineering University, Yantai, China

3 Photonics and Optical Communications, School of Electrical Engineering and Telecommunications, University of New South Wales, Sydney, NSW, Australia

*Address all correspondence to: zhangjianzhong@hrbeu.edu.cn

IntechOpen

© 2022 The Author(s). Licensee IntechOpen. This chapter is distributed under the terms of the Creative Commons Attribution License (<http://creativecommons.org/licenses/by/3.0>), which permits unrestricted use, distribution, and reproduction in any medium, provided the original work is properly cited. 

References

- [1] Kao KC, Hockham GA. Dielectric-fibre surface waveguides for optical frequencies. *Proceedings of the Institution of Electrical Engineers*. 1966;**113**:1151-1158. DOI: 10.1049/ piee.1966.0189
- [2] Kao KC. Nobel Lecture: Sand from centuries past: Send future voices fast. *Reviews of Modern Physics*. 2010;**82**:2299. DOI: 10.1103/ RevModPhys.82.2299
- [3] Press release. NobelPrize.org. [Internet]. 2009. Available from: <https://www.nobelprize.org/prizes/physics/2009/press-release/>
- [4] Kapron FP, Donald BK, Maurer RD. Radiation losses in glass optical waveguides. *Applied Physics Letters*. 1970;**17**:423-425. DOI: 10.1063/1.1653255
- [5] MacChesney JB, O'connor PB, Presby HM. A new technique for the preparation of low-loss and graded-index optical fibers. *Proceedings of the IEEE*. 1974;**62**:1280-1281. DOI: 10.1109/ PROC.1974.9608
- [6] Recipients of the Charles Stark Draper Prize [Internet]. 1999. Available from: <https://www.nae.edu/55048/page1999>
- [7] Zhou P, Wang X, Xiao H, Ma Y, Chen J. Review on recent progress on Yb-doped fiber laser in a variety of oscillation spectral ranges. *Laser Physics*. 2012;**22**:823-831. DOI: 10.1134/S1054660X12050404
- [8] Bradley JDB, Pollnau M. Erbium-doped integrated waveguide amplifiers and lasers. *Laser & Photonics Reviews*. 2011;**5**:368-403. DOI: 10.1002/lpor.201000015
- [9] Sincore A, Bradford JD, Cook J, Shah L, Richardson MC. High average power thulium-doped silica fiber lasers: Review of systems and concepts. *IEEE Journal of Selected Topics in Quantum Electronics*. 2017;**24**:1-8. DOI: 10.1109/JSTQE.2017.2775964
- [10] Zhou P, Wang X, Ma Y, Lv H, Liu Z. Review on recent progress on mid-infrared fiber lasers. *Laser Physics*. 2012;**22**:1744-1751. DOI:10.1134/S1054660X12110199
- [11] Dianov EM. Bismuth-doped optical fibers: A challenging active medium for near-IR lasers and optical amplifiers. *Light: Science & Applications*. 2012;**1**:e12-e12. DOI: 10.1038/lsa.2012.12
- [12] Luo Y, Wen J, Zhang J, Canning J, Peng GD. Bismuth and erbium codoped optical fiber with ultrabroadband luminescence across O-, E-, S-, C-, and L-bands. *Optics Letters*. 2012;**37**:3447-3449. DOI: 10.1364/OL.37.003447
- [13] Luo Y, Yan B, Zhang J, Wen J, He J, Peng GD. Development of Bi/Er co-doped optical fibers for ultra-broadband photonic applications. *Frontiers of Optoelectronics*. 2018;**11**:37-52. DOI: 10.1007/s12200-017-0764-y
- [14] Xiao L, Demokan MS, Jin W, Wang Y, Zhao CL. Fusion splicing photonic crystal fibers and conventional single-mode fibers: Microhole collapse effect. *Journal of Lightwave Technology*. 2007;**25**:3563-3574. DOI: 10.1109/JLT.2007.907787
- [15] Vienne G, Xu Y, Jakobsen C, Deyerl HJ, Jensen JB, Sørensen T, et al. Ultra-large bandwidth hollow-core guiding in all-silica Bragg fibers with nano-supports. *Optics Express*.

2004;**12**:3500-3508. DOI: 10.1364/OPEX.12.003500

[16] Newkirk AV, Lopez JEA, Correa RA, Schülzgen A, Mazurowski J. Anti-resonant hollow core fiber for precision timing applications. In: *Astronomical Optics: Design, Manufacture, and Test of Space and Ground Systems*. International Society for Optics and Photonics. San Diego, California, United States: SPIE; 2017. p. 104010F

[17] Geittner P, Kuppers D, Lydtin H. Low-loss optical fibers prepared by plasma-activated chemical vapor deposition (CVD). *Applied Physics Letters*. 1976;**28**:645-646. DOI: 10.1063/1.88608

[18] Schultz PC. Fabrication of optical waveguides by the outside vapor deposition process. *Proceedings of the IEEE*. 1980;**68**:1187-1190. DOI: 10.1109/PROC.1980.11828

[19] Izawa T, Sudo S, Hanawa F. Continuous fabrication process for high-silica fiber preforms. *IEICE Transactions*. 1979;**62**:779-785. DOI: naid/10010177421

[20] Knight JC, Birks TA, Russell PSJ, Atkin DM. All-silica single-mode optical fiber with photonic crystal cladding. *Optics Letters*. 1996;**21**:1547-1549. DOI: 10.1364/OL.21.001547

[21] Layani M, Wang X, Magdassi S. Novel materials for 3D printing by photopolymerization. *Advanced Materials*. 2018;**30**(41): 1706344. DOI: 10.1002/adma.201706344

[22] Kruth JP, Mercelis P, Van Vaerenbergh J, Froyen L, Rombouts M. Binding mechanisms in selective laser sintering and selective laser melting. *Rapid Prototyping Journal*. 2005;**11**:26-36. DOI: 10.1108/13552540510573365

[23] Tang Y, Futh JYH, Loh HT, Wong YS, Lu L. Direct laser sintering of a silica sand. *Materials and Design*. 2003;**24**:623-629. DOI: 10.1016/S0261-3069(03)00126-2

[24] Klocke F, Wirtz H. Selective laser sintering of zirconium silicate. *Proceedings of Solid Freeform Fabrication Symposium*. 1998:605-612. DOI: 10.26153/tsw/652

[25] Klocke F, McClung A, Ader C. Direct laser sintering of borosilicate glass. *Proceedings of Solid Freeform Fabrication Symposium*. 2004:214-219. DOI: 10.26153/tsw/6986

[26] Kruth JP, Wang X, Laoui T, Froyen L. Lasers and materials in selective laser sintering. *Assembly Automation*. 2003;**23**:357-371. DOI: 10.1108/01445150310698652

[27] Song JL, Li YT, Deng QL, Hu DJ. Rapid prototyping manufacturing of silica sand patterns based on selective laser sintering. *Journal of Materials Processing Technology*. 2007;**187-188**:614-618. DOI: 10.1016/j.jmatprotec.2006.11.108

[28] Klein J, Stern M, Franchin G, Kayser M, Inamura C, Dave S, et al. Additive manufacturing of optically transparent glass. *3D Printing and Additive Manufacturing*. 2015;**2**:92-105. DOI: 10.1089/3dp.2015.0021

[29] Gaynor AT, Guest JK. Topology optimization considering overhang constraints: Eliminating sacrificial support material in additive manufacturing through design. *Structural and Multidisciplinary Optimization*. 2016;**54**:1157-1172. DOI: 10.1007/s00158-016-1551-x

[30] Zwier MP, Wits WW. Design for additive manufacturing: Automated

build orientation selection and optimization. *Procedia CIRP*. 2016;**55**:128-133. DOI: 10.1016/j.procir.2016.08.040

[31] Yu EA, Yeom J, Tutum CC, Vouge E, Miikkulainen R. Evolutionary decomposition for 3D printing. *GECCO'17: Proceedings of the Genetic and Evolutionary Computation Conference*. 2017:1272-1279. DOI: 10.1145/3071178.3071310

[32] Cruz A, Cordeiro C, Franco M. 3D printed hollow-core terahertz fibers. *Fibers*. 2018;**6**(3):43. DOI: 10.3390/fib6030043

[33] Sung C, Fang N, Wu DM, Zhang X. Projection micro-stereolithography using digital micro-mirror dynamic mask. *Sensors and Actuators A: Physical*. 2005;**121**:113-120. DOI: 10.1016/j.sna.2004.12.011

[34] Wu D, Zhao Z, Zhang Q, Qi HJ, Fang D. Mechanics of shape distortion of DLP 3D printed structures during UV post-curing. *Soft Matter*. 2019;**15**:6151-6159. DOI: 10.1039/c9sm00725c

[35] Komissarenko D, Sokolov P, Evstigneeva A, Shmeleva I, Dosovitsky A. Rheological and curing behavior of acrylate-based suspensions for the DLP 3D printing of complex zirconia parts. *Materials*. 2018;**11**:2350. DOI: 10.3390/ma1122350

[36] Meisel NA, Gaynor A, Williams CB, Guest JK. Multiple-material topology optimization of compliant mechanisms created via polyjet 3d printing. In: *Proceedings of the 24th Annual international solid freeform fabrication symposium an additive manufacturing conference*; University of Texas at Austin; 2013; p. 980-997. DOI: 10.26153/tsw/15651

[37] Peng GD, Luo Y, Zhang J, Wen J, Chu Y, Cook K, et al. 3D silica lithography for future optical fiber fabrication. In: *Handbook of Optical Fibers*. Singapore: Springer Singapore; 2019. pp. 637-653. DOI: 10.1007/978-981-10-7087-7_79

[38] Anuszkiewicz A, Kasztelaniec R, Filipkowski A, Stepniewski G, Stefaniuk T, Siwicki B, et al. Fused silica optical fibers with graded index nanostructured core. *Scientific Reports*. 2018;**8**:12329. DOI: 10.1038/s41598-018-30284-1

[39] Cook K, Canning J, Leon-Saval S, Reid Z, Hossain MA, Comatti JE, et al. Air-structured optical fiber drawn from a 3D-printed preform. *Optics Letters*. 2015;**40**:3966-3969. DOI: 10.1364/ol.40.003966

[40] Li J, Nallappan K, Guerboukha H, Skorobogatiy M. 3D printed hollow core terahertz Bragg waveguides with defect layers for surface sensing applications. *Optics Express*. 2017;**25**:4126-4144. DOI: 10.1364/oe.25.004126

[41] Yang J, Zhao J, Gong C, Tian H, Sun L, Chen P, et al. 3D printed low-loss THz waveguide based on Kagome photonic crystal structure. *Optics Express*. 2016;**24**:22454-22460. DOI: 10.1364/oe.24.022454

[42] Van Putten LD, Gorecki J, Numkam Fokoua E, Apostolopoulos V, Poletti F. 3D-printed polymer antiresonant waveguides for short-reach terahertz applications. *Applied Optics*. 2018;**57**:3953-3958. DOI: 10.1364/ao.57.003953

[43] Li J, Ma T, Nallapan K, Guerboukha H, Skorobogatiy M. 3D printed hollow core terahertz Bragg waveguides with defect layers for surface sensing applications. In: 2017 42nd International Conference on

- Infrared, Millimeter, and Terahertz Waves (IRMMW-THz). IEEE: Cancun, Mexico; 2017. DOI: 10.1109/irmmw-thz.2017.8066908
- [44] Cook K, Balle G, Canning J, Chartier L, Athanaze T, Hossain MA, et al. Step-index optical fiber drawn from 3D printed preforms. *Optics Letters*. 2016;**41**:4554-4557. DOI: 10.1364/ol.41.004554
- [45] Kaufman JJ, Bow C, Tan FA, Cole AM, Abouraddy AF. 3D printing preforms for fiber drawing and structured functional particle production. In: *Proceedings of the Australian Conference on Optical Fibre Technology*. Optical Society of America. 2016. DOI: 10.1364/ACOFT.2016.AW4C.1
- [46] Hong B, Swithenbank M, Greenall N, Clarke RG, Chudpooti N, Akkaraekthalin P, et al. Low-loss asymptotically single-mode THz Bragg fiber fabricated by digital light processing rapid prototyping. *IEEE Transactions on Terahertz Science and Technology*. 2018;**8**:90-99. DOI: 10.1109/tthz.2017.2778047
- [47] Kotz F, Plewa K, Bauer W, Schneider N, Keller N, Nargang T, et al. Liquid glass: A facile soft replication method for structuring glass. *Advanced Materials*. 2016;**28**:4646-4650. DOI: 10.1002/adma.201506089
- [48] Kotz F, Schneider N, Striegel A, Wolfschläger A, Keller N, Worgull M, et al. Glassomer—Processing fused silica glass like a polymer. *Advanced Materials*. 2018;**30**:1707100. DOI: 10.1002/adma.201707100
- [49] Kotz F, Arnold K, Bauer W, Schild D, Keller N, Sachsenheimer K, et al. Three-dimensional printing of transparent fused silica glass. *Nature*. 2017;**544**:337-339. DOI: 10.1038/nature22061
- [50] Moore DG, Barbera L, Masania K, Studart AR. Three-dimensional printing of multicomponent glasses using phase-separating resins. *Nature Materials*. 2019;**19**(2):212-217. DOI: 10.1038/s41563-019-0525-y
- [51] Nguyen DT, Meyers C, Yee TD, Dudukovic NA, Destino JF, Zhu C, et al. 3D-printed transparent glass. *Advanced Materials*. 2017;**29**:1701181. DOI: 10.1002/adma.201701181
- [52] Destino JF, Dudukovic NA, Johnson MA, Nguyen DT, Yee TD, Egan GC, et al. 3D printed optical quality silica and silica-titania glasses from sol-gel feedstocks. *Advanced Materials Technologies*. 2018;**3**:1700323. DOI: 10.1002/admt.201700323
- [53] Sasan K, Lange A, Yee TD, Dudukovic NA, Nguyen DT, Johnson MA, et al. Additive manufacturing of optical quality germania-silica glasses. *ACS Applied Materials & Interfaces*. 2020;**12**:6736-6741. DOI: 10.1021/acsami.9b21136
- [54] Chu Y, Fu X, Luo Y, Canning J, Tian Y, Cook K, et al. Silica optical fiber drawn from 3D printed preforms. *Optics Letters*. 2019;**44**:5358-5361. DOI: 10.1364/OL.44.005358
- [55] Chu Y, Fu X, Luo Y, Canning J, Wang J, Ren J, et al. Additive manufacturing fiber preforms for structured silica fibers with bismuth and erbium dopants. *Light. Advanced Manufacturing*. 2022;**3**:1-7. DOI: 10.37188/lam.2022.021
- [56] Zheng B, Yang J, Qi F, Wang J, Zhang X, Wang P. Fabrication of Yb-doped silica micro-structured optical fibers from UV-curable nano-composites and their application in temperature sensing. *Journal of Non-Crystalline Solids*. 2021;**573**:121129. DOI: 10.1016/j.jnoncrysol.2021.121129

[57] Rosales ALC, Núñez-Velázquez MMA, Sahu JK. 3D printed Er-doped silica fibre by direct ink writing. *Proceedings of the EPJ Web of Conferences*. 2020;**243**:20002.
DOI: 10.1051/epjconf/202024320002

[58] Camacho-Rosales A, Núñez-Velázquez MMA, Zhao X, Yang S, Sahu JK. Development of 3-D printed silica preforms. In: 2019 Conference on Lasers and Electro-Optics Europe & European Quantum Electronics Conference (CLEO/Europe-EQEC). 2019.
DOI: 10.1109/cleoe-eqec.2019.8871436

[59] Rosales ALC, Núñez-Velázquez MMA, Zhao X, Sahu JK. Optical fibers fabricated from 3D printed silica preforms. *Proceedings of the Laser 3D Manufacturing VII*. 2020;**11271**:112710U.
DOI: 10.1117/12.2543210

[60] Liu C, Qian B, Liu X, Tong L, Qiu J. Additive manufacturing of silica glass using laser stereolithography with a top-down approach and fast debinding. *RSC Advances*. 2018;**8**:16344-16348.
DOI: 10.1039/c8ra02428f